Hindawi Publishing Corporation
Journal of Control Science and Engineering
Volume 2016, Article ID 7256039, 11 pages
http://dx.doi.org/10.1155/2016/7256039

Research Article

H_∞ Optimal Inversion Feedforward and Robust Feedback Based 2DOF Control Approach for High Speed-Precision Positioning Systems

Chao Peng,[1,2] Chongwei Han,[2] Jianxiao Zou,[1] and Guanghui Zhang[2]

[1] *School of Mechanical Engineering, University of Electronic Science and Technology of China, Chengdu, Sichuan 611731, China*
[2] *Northwest Institute of Mechanical & Electrical Engineering, Xianyang, Shanxi 712099, China*

Correspondence should be addressed to Chao Peng; pcddiy@163.com

Received 24 July 2015; Revised 30 October 2015; Accepted 10 November 2015

Academic Editor: Petko Petkov

This paper proposed a novel H_∞ optimal inversion feedforward and robust feedback based two-freedom-of-freedom (2DOF) control approach to address the positioning error caused by system uncertainties in high speed-precision positioning system. To minimize the H_∞ norm of the positioning error in the presence of model uncertainty, a linear matrix inequality (LMI) synthesis approach for optimal inversion feedforward controller design is presented. The specification of position resolution, control width, robustness, and output signal magnitude imposed on the entire 2DOF control system are taken as optimization objectives of feedback controller design. The robust feedback controller design approach integrates with feedforward controller systematically and is obtained via LMI optimization. The proposed approach was illustrated through a simulation example of nanopositioning control in atomic force microscope (AFM); the experiment results demonstrated that the proposed 2DOF control approach not only achieves the performance specification but also could improve the positioning control performance compared with H_∞ mixed sensitivity feedback control and inversion-based 2DOF control.

1. Introduction

The performance of high speed-precision positioning system such as piezoelectric and precision motor actuated system is required to meet the specification in scanning probe microscopy (SPM) [1, 2], microelectromechanical system [3, 4], optical-hard disk drive [5, 6], and so on. The positioning control performance could be characterized by positioning resolution, control bandwidth, and system robustness [1–6]. Various feedback control approaches have been studied and demonstrated that it could render requirements on positioning resolution and robustness satisfied at low frequencies [7–9]. However, the positioning resolution and control bandwidth of feedback control are limited for the Bode Sensitivity Integral theorem [10, 11]. It has been demonstrated that the feedforward control could increase the feedback control bandwidth [12, 13]. To improve the system positioning control performance, considerable 2DOF control approaches which combine the feedforward controller and feedback controller have been studied [14–18].

The inversion control technology could achieve exact trajectory tracking and precision positioning for linear and nonlinear system without system uncertainty [19, 20]. The stable-inversion [21], preview-based optimal inversion [22], and inversion-based iterative control [23] approach have improved the practicality of inversion technology. However, the positioning control performance of inversion feedforward control is limited by modeling uncertainties and disturbances [24]. Thus, recently, the inversion feedforward based 2DOF control approaches which utilize the robust feedback control to compensated the limitation of inversion feedforward controller have been presented and demonstrated that they could achieve good positioning performance [25–27]. However, the feedforward controller and feedback controller in the above 2DOF control approaches are designed separately; the feedback controller is designed by conventional

H_∞ mixed sensitivity feedback control approach without taking the effect of feedforward controller into account. There exist challenges in inversion feedforward based 2DOF control: (1) inversion feedforward controller design optimization with considering the system uncertainty and (2) how to integrate the feedforward controller and feedback controller design systematically to obtain the desired requirement positioning resolution, control bandwidth, and robustness of the entire 2DOF control system.

To minimize the adverse effect caused by system uncertainties and make the requirements of performance of the entire 2DOF control system satisfied, a novel H_∞ optimal inversion feedforward and robust feedback based 2DOF control approach is proposed in this paper. The main contribution of this paper is as follows. (1) A new LMI representation for H_∞ optimal inversion feedforward controller design which takes minimizing the H_∞ norm of the positioning error caused by feedforward control in presence of the system uncertainty as optimization objective. (2) A 2DOF control positioning performance optimization problem based on H_∞ mixed sensitivity is formulated and a LMI optimization based robust feedback controller design approach integrating with feedforward controller systematically. The proposed 2DOF control design approach is evaluated through the experiment.

The rest of this paper is organized as follows. The design objective of H_∞ optimal inversion feedforward and robust feedback based 2DOF control is formulated in Section 2. In Section 3, the LMI based H_∞ optimal inversion feedforward controller design approach is presented. The design of robust feedback controller is given in Section 4. The proposed 2DOF control approach is illustrated through AFM simulation experiment in Section 5. Finally, the conclusion is discussed in Section 6.

2. Problem Formulation

2.1. System Description. Consider the SISO LTI system with parameter uncertainty:

$$G(s) = p(s,\theta) = \frac{n(s,\theta)}{d(s,\theta)}, \tag{1}$$

where $n(s,\theta)$ and $d(s,\theta)$ are polynomials of Laplace variable s and $\theta = \{\theta_1, \theta_2, \ldots, \theta_q\} \in \mathbb{R}^q$ is the uncertain parameter vector that parameterizes the transfer function $G(s)$.

Defining the nominal parameter vector of θ as $\theta_m = \{\theta_{m1}, \theta_{m2}, \ldots, \theta_{mq}\}$, the nominal model of the system could be denoted as $G_m(s) = p(s,\theta_m)$.

We assume that θ is known to lie in a box domain Ω which is defined as

$$\begin{aligned}\Omega &= \left\{\theta \mid \theta_i = \theta_{m_i} + \Delta\theta_i,\ \Delta\theta_i \in [a_i, b_i],\ i = 1, 2, \ldots, q\right\},\end{aligned} \tag{2}$$

where $\Delta\theta_i$ are the variation of θ_i.

Assumption 1. System $G(s)$ is invertible, and the relative degree of $G(s)$ is at least two (i.e., has at least two more poles than zeros). System $G(s)$ and its inverse $G^{-1}(s)$ are hyperbolic; that is, $G(s)$ does not have poles or zeros on the imaginary axis of the complex plane.

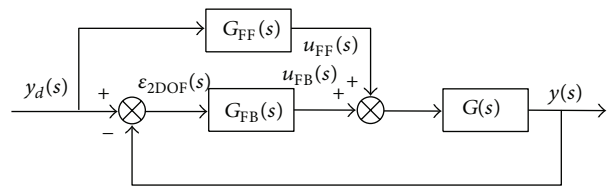

Figure 1: Block diagram of 2DOF control system.

Remark 2. The requirements that the system $G(s)$ is invertible and hyperbolic and that the relative degree of $G(s)$ is more than one are needed for computation [21] and robustness [22] of the exact inverse.

2.2. H_∞ Optimal Inversion Feedforward and Robust Feedback Based 2DOF Control. Consider the 2DOF control system shown in Figure 1. In this figure, $G(s)$ is the transfer function of a LTI plant as described in (1), $G_{FF}(s)$ and $G_{FB}(s)$ are feedforward controller and feedback controller, respectively. The signal $y_d(s)$ represents the desired outputting and $u(s)$ represents the input to the plant $G(s)$. The signal $y(s)$ represents the actual output of the entire 2DOF control system.

The transfer function from the desired trajectory $y_d(s)$ to actual outputs $y(s)$ and $G_{2DOF}(s)$ is given by

$$G_{2DOF}(s) = \left[G_{FF}(s) + G_{FB}(s)\right] G(s) S(s), \tag{3}$$

where $S(s)$ is the feedback sensitivity function; that is,

$$S(s) = \left(1 + G(s) G_{FB}(s)\right)^{-1}. \tag{4}$$

The outputting error of entire 2DOF control system $\varepsilon_{2DOF}(s)$ can be decoupled as multiplication of the feedforward path outputting error $\varepsilon_{FF}(s)$ and the feedback sensitivity function $S(s)$:

$$\begin{aligned}\varepsilon_{2DOF}(s) &= 1 - G_{2DOF}(s) = \left(1 - G(s) G_{FF}(s)\right) S(s) \\ &\triangleq \varepsilon_{FF}(s) S(s).\end{aligned} \tag{5}$$

Remark 3. By Bode Sensitivity Integral theorem, the small feedforward path output error could improve the bandwidth of feedback control and output error. If $G_{FF}(s) = G^{-1}(s)$, the output error could be zero; however, it is impossible to find the exact inverse of the system for the modeling uncertainty.

The control block and output error of the 2DOF control system are now presented. The design goal of H_∞ optimal feedforward and robust feedback based 2DOF control design is to make the following two optimization objects satisfied.

(1) Find an H_∞ optimal robust inversion-based feedforward controller $G^*_{FF}(s)$ to minimize the H_∞ norm of feedforward path output error in the presence of system uncertainties; that is,

$$G^*_{FF}(s) = \arg\min_{G_{FF}} \sup_{\theta\in\Omega} \left\|\varepsilon_{FF}(s)\right\|_\infty. \tag{6}$$

(2) After determining the feedforward controller $G_{\mathrm{FF}}^{*}(s)$, find a robust feedback controller $G_{\mathrm{FB}}^{*}(s)$ to minimize the H_∞ norm of transfer function $\Phi(G_{\mathrm{FB}})$; that is,

$$G_{\mathrm{FB}}^{*}(s) = \arg\min_{G_{\mathrm{FB}}} \sup_{\theta\in\Omega} \left\|\Phi\left(G_{\mathrm{FB}}\right)\right\|_\infty, \tag{7}$$

where

$$\left\|\Phi\left(G_{\mathrm{FB}}\right)\right\|_\infty = \left\| \begin{matrix} W_p(s) S_{2\mathrm{DOF}}(s) \\ W_u(s) S_{2\mathrm{DOF}}(s) G_{\mathrm{FB}}(s) \\ W_t(s) T_{2\mathrm{DOF}}(s) \end{matrix} \right\|_\infty. \tag{8}$$

$W_p(s)$ denotes the weighting function for output bandwidth and output error limitation, $W_t(s)$ denotes the weighting function for robustness performance of system, $W_u(s)$ denotes the weighting function for magnitude of output signal of feedback controller, and $S_{2\mathrm{DOF}}(s)$ and $T_{2\mathrm{DOF}}(s)$ are the transfer function from desired trajectory $y_d(s)$ to output error and $\varepsilon_{2\mathrm{DOF}}(s)$ and $y_d(s)$ to actual output $y(s)$.

3. H_∞ Optimal Inversion Feedforward Controller Design

This section is devoted to H_∞ optimal inversion feedforward controller design. At first feedforward controller based on H_∞ optimal inverse of $G(s)$ is designed by LMI optimization, and then the feedforward controller is implemented by preview-based inversion [21].

3.1. H_∞ Optimal Inversion of System. A modulation function $a(s)$ is introduced to inversion feedforward controller design as follows:

$$G_{\mathrm{FF}}(s) = a(s) G_m^{-1}(s) \triangleq a(s) \widehat{G}(s). \tag{9}$$

Consider Assumption 1; $\widehat{G}(s)$ is improper; that is, the poles number is less than zeros number. Assume $a(s)$ is proper; thus, inversion feedforward controller also could be decoupled as proper element $\widehat{G}_{\mathrm{impr}}(s)$:

$$\begin{aligned} G_{\mathrm{FF}}(s) &= a(s)\widehat{G}(s) = a(s)\frac{N_m(s)}{\mathrm{den}_m(s)} \\ &= a(s)\frac{A_m(s)}{\mathrm{den}_m(s)} B_m(s) \triangleq a(s)\widehat{G}_{\mathrm{pr}}(s) B_m(s) \\ &\triangleq a(s)\widehat{G}_{\mathrm{pr}}(s)\widehat{G}_{\mathrm{impr}}(s) \triangleq \widehat{G}_a(s)\widehat{G}_{\mathrm{impr}}(s), \end{aligned} \tag{10}$$

where $\mathrm{den}_m(s)$ and $N_m(s)$ are the denominator and numerator of $\widehat{G}(s)$, respectively, The order of $A_m(s)$ is equivalent to the order of $\mathrm{den}_m(s)$. Thus, the relative degree of $\widehat{G}_{\mathrm{pr}}(s)$ is zero and the order of $\widehat{G}_{\mathrm{impr}}(s)$ is equal to the relative degree of nominal model $G_m(s)$.

The transfer function of feedforward path output error $\varepsilon_{\mathrm{FF}}(s)$ could be rewritten as

$$\begin{aligned} \varepsilon_{\mathrm{FF}}(s) &= 1 - G_{\mathrm{FF}}(s) G(s) = 1 - \widehat{G}_a(s)\widehat{G}_{\mathrm{impr}}(s) G(s) \\ &\triangleq 1 - \widehat{G}_a(s)\widetilde{G}(s). \end{aligned} \tag{11}$$

Remark 4. Because the order of $\widehat{G}_{\mathrm{impr}}(s)$ is equal to the relative degree of nominal model $G_m(s)$, the relative degree of $\widetilde{G}(s)$ is equal to zero. The modulation function $a(s)$ could be obtained as $a(s) = \widehat{G}_a(s)/\widehat{G}_{\mathrm{pr}}(s)$.

Now, a proper transfer function $\widetilde{G}(s)$ whose relative degree is zero can be obtained by multiplying improper element $\widehat{G}_{\mathrm{impr}}(s)$ with $G(s)$. Consider the parameter uncertainty domain of $G(s)$, the parameters of $\widetilde{G}(s)$ can also be known to lie in a box uncertainty domain, and the state space matrices of $\widetilde{G}(s)$ which depend on θ [28, 29]. The sate space representation of $\widetilde{G}(s)$ can be given as

$$\begin{aligned} \dot{\tilde{x}} &= \widetilde{A}(\theta)\tilde{x} + \widetilde{B}(\theta)\tilde{u}, \\ \tilde{y} &= \widetilde{C}(\theta)\tilde{x} + \widetilde{D}(\theta)\tilde{u}. \end{aligned} \tag{12}$$

The state space representation of $\widehat{G}_a(s)$ is given as

$$\begin{aligned} \dot{\hat{x}}_a &= \widehat{A}_a\hat{x}_a + \widehat{B}_a\hat{u}_a, \\ \hat{y}_a &= \widehat{C}_a\hat{x}_a + \widehat{D}_a\hat{u}_a. \end{aligned} \tag{13}$$

Now, the state space representation of the feedforward path output error $\varepsilon_{\mathrm{FF}}(s)$ can be written as

$$\begin{aligned} \dot{x}_{\varepsilon_{\mathrm{FF}}} &= A_{\varepsilon_{\mathrm{FF}}} x_{\varepsilon_{\mathrm{FF}}} + B_{\varepsilon_{\mathrm{FF}}} u_{\varepsilon_{\mathrm{FF}}}, \\ y_{\varepsilon_{\mathrm{FF}}} &= C_{\varepsilon_{\mathrm{FF}}} x_{\varepsilon_{\mathrm{FF}}} + D_{\varepsilon_{\mathrm{FF}}} u_{\varepsilon_{\mathrm{FF}}}, \end{aligned} \tag{14}$$

where the state space matrices are given by

$$\begin{aligned} A_{\varepsilon_{\mathrm{FF}}}(\theta) &= \begin{bmatrix} \widetilde{A}(\theta) & \widetilde{B}(\theta)\widehat{C}_a \\ 0 & \widehat{A}_a \end{bmatrix}, \\ B_{\varepsilon_{\mathrm{FF}}}(\theta) &= \begin{bmatrix} \widetilde{B}(\theta)\widehat{D}_a \\ \widehat{B}_a \end{bmatrix}, \\ C_{\varepsilon_{\mathrm{FF}}}(\theta) &= \begin{bmatrix} -\widetilde{C}(\theta) & -\widetilde{D}(\theta)\widehat{C}_a \end{bmatrix}, \\ D_{\varepsilon_{\mathrm{FF}}}(\theta) &= 1 - \widetilde{D}(\theta)\widehat{D}_a. \end{aligned} \tag{15}$$

The objective of the inversion feedforward controller design in (6) could be transformed to find an optimal function; that is,

$$\begin{aligned} \widehat{G}_a^{*}(s) &= \min_{\widehat{G}_a} \sup_{\theta\in\Omega} \left(\left\|\varepsilon_{\mathrm{FF}}(s)\right\|_\infty\right) \\ &= \min_{\widehat{G}_a} \sup_{\theta\in\Omega} \left(\left\|1 - \widehat{G}_a(s)\widetilde{G}(s)\right\|_\infty\right). \end{aligned} \tag{16}$$

The bounded real lemma (BRL) [30] will be utilized for solving the optimal $\widehat{G}_a(s)$. The LMI representation lemma is given as follows.

Lemma 5. *A proper element in inversion feedforward controller $G_{FF}(s)$ as in (10) is the solution to the minimization problem in (16) whose state space matrices $\widehat{A}_a, \widehat{B}_a, \widehat{C}_a$, and $\widehat{D}_a$ and a symmetric matrix $V > 0$ could minimize the scale*

γ in presence of uncertain parameters, subjected to following parameterized LMI, that is,

$$\min_{\widehat{A}_a,\widehat{B}_a,\widehat{C}_a,\widehat{D}_a,V}\left(\max_{\theta}(\gamma)\right) \tag{17}$$

subject to

$$\begin{bmatrix} VA_{\varepsilon_{FF}}(\theta)+A^T_{\varepsilon_{FF}}(\theta)V & VB_{\varepsilon_{FF}}(\theta) & C^T_{\varepsilon_{FF}}(\theta) \\ B^T_{\varepsilon_{FF}}(\theta)V & -\gamma^2 I & D^T_{\varepsilon_{FF}}(\theta) \\ C_{\varepsilon_{FF}}(\theta) & D_{\varepsilon_{FF}}(\theta) & -I \end{bmatrix} < 0, \quad \theta\in\Omega. \tag{18}$$

Proof. Consider the uncertainty domain Ω and bounded real lemma; if there exist a positive-definite symmetric matrix V and matrices $\widehat{A}_a, \widehat{B}_a, \widehat{C}_a$, and $\widehat{D}_a$ which could render the parameterized LMIs in (18) satisfied, H_∞ norm of feedforward path positioning error is less than γ in the presence of uncertain parameters θ; that is, $\|\varepsilon_{\mathrm{FF}}(s)\|_\infty < \gamma,\ \theta\in\Omega$.

Thus, if matrices $\widehat{A}_a, \widehat{B}_a, \widehat{C}_a$, and $\widehat{D}_a$ and a given $\widehat{G}_a(s)$ and V could satisfy the optimization objective in (17), a solution for minimizing problem in (16) $\widehat{G}^*_a(s)$ exists. This completes the proof. □

The solution to the optimization problem in (6) could be given by the following theorem.

Theorem 6. *Assume the H_∞ optimal inversion feedforward controller $G^*_{FF}(s)$ with form as (10) is $G^*_{FF}(s)=\widehat{G}^*_a(s)\widehat{G}_{impr}(s)$.*

(a) The controller $G^*_{FF}(s)$ that could solve the minimization problem in (6) exits, if there exists a solution $(X,Y,Z,U,W_{11},\widehat{V}_{11})$ where $W_{11}=W^T_{11}>0$, $\widehat{V}_{11}=\widehat{V}^T_{11}>0$ for $\theta\in\Omega$ for the following optimization:

$$\min_{X,Y,Z,U,W_{11},\widehat{V}_{11}}\left(\max_{\theta}(\gamma)\right) \tag{19}$$

subject to

$$\begin{bmatrix} \widetilde{A}(\theta)\widehat{V}^T_{11}+\widehat{V}_{11}\widetilde{A}^T(\theta) & \widetilde{A}(\theta)W_{11}+\widetilde{B}(\theta)Z+X+\widehat{V}_{11}\widetilde{A}^T(\theta) & \widetilde{B}(\theta)U+Y & -\widehat{V}_{11}\widetilde{C}^T(\theta) \\ * & \widetilde{A}(\theta)W_{11}+\widetilde{B}(\theta)Z+\left(\widetilde{A}(\theta)W_{11}\right)^T+\left(\widetilde{B}(\theta)Z\right)^T & \widetilde{B}(\theta)U & -W_{11}\widetilde{C}^T(\theta)-Z^T\widetilde{D}^T(\theta) \\ * & * & -\gamma^2 I & I-\left(\widetilde{D}(\theta)U\right)^T \\ * & * & * & -I \end{bmatrix} < 0. \tag{20}$$

(b) The proper element in $G^*_{FF}(s)$, $\widehat{G}^*_a(s)$, is given as follows:

$$\begin{aligned} \widehat{A}^*_a &= V^{-1}_{12}V_{11}X\left(W^T_{12}\right)^{-1}, \\ \widehat{B}^*_a &= V^{-1}_{12}V_{11}Y, \\ \widehat{C}^*_a &= Z\left(W^T_{12}\right)^{-1}, \\ \widehat{D}^*_a &= U. \end{aligned} \tag{21}$$

Considering the partition of $A_{\varepsilon_{FF}}$ and $B_{\varepsilon_{FF}}$, we introduce a partition of V and its inverse $W\triangleq V^{-1}$:

$$\begin{aligned} V &= \begin{bmatrix} V_{11} & V_{12} \\ V^T_{12} & V_{22} \end{bmatrix}, \\ W &= \begin{bmatrix} W_{11} & W_{12} \\ W^T_{12} & W_{22} \end{bmatrix}. \end{aligned} \tag{22}$$

Since $WV=I$,

$$\begin{aligned} W_{11}V_{11}+W_{12}V^T_{12} &= I, \\ W_{11}V_{12}+W_{12}V_{22} &= 0. \end{aligned} \tag{23}$$

Define a full ranked and square matrix, which will be used in following matrix inequalities transformation:

$$F\triangleq\begin{bmatrix} V^{-1}_{11} & 0 \\ W_{11} & W_{12} \end{bmatrix}\triangleq\begin{bmatrix} \widehat{V}_{11} & 0 \\ W_{11} & W_{12} \end{bmatrix}. \tag{24}$$

To obtain a feasible solution which could render the LMIs in (18) satisfied and consider the partition of V in (22), we introduce full ranked matrices X,Y,Z, and U and assume $\widehat{A}_a, \widehat{B}_a, \widehat{C}_a$, and $\widehat{D}_a$ have following form:

$$\begin{aligned} \widehat{A}_a &= V^{-1}_{12}V_{11}X\left(W^T_{12}\right)^{-1}, \\ \widehat{B}_a &= V^{-1}_{12}V_{11}Y, \\ \widehat{C}_a &= Z\left(W^T_{12}\right)^{-1}, \\ \widehat{D}_a &= U. \end{aligned} \tag{25}$$

Multiplying the inequalities in (18) by $\mathrm{diag}\{F, I, I\}$ *and* $\mathrm{diag}\{F^T, I, I\}$ *on the left and on the right, respectively, we obtain the following LMI:*

$$\begin{bmatrix} FVA_{\varepsilon_{FF}}(\theta)F^T + FA^T_{\varepsilon_{FF}}(\theta)VF^T & FVB_{\varepsilon_{FF}}(\theta) & FC^T_{\varepsilon_{FF}}(\theta) \\ B^T_{\varepsilon_{FF}}(\theta)VF^T & -\gamma I & D^T_{\varepsilon_{FF}}(\theta) \\ C_{\varepsilon_{FF}}(\theta)F^T & D_{\varepsilon_{FF}}(\theta) & -\gamma I \end{bmatrix} < 0. \tag{26}$$

Now, the LMI item in (26) could be written as

$$\begin{aligned} FVA_{\varepsilon_{FF}}(\theta)F^T &= \begin{bmatrix} \widetilde{A}(\theta)\widehat{V}^T_{11} & \widetilde{A}(\theta)W_{11} + \widetilde{B}(\theta)Z + X \\ \widetilde{A}(\theta)\widehat{V}^T_{11} & \widetilde{A}(\theta)W_{11} + \widetilde{B}(\theta)Z \end{bmatrix}, \\ FVB_{\varepsilon_{FF}} &= \begin{bmatrix} \widetilde{B}(\theta)\widehat{D}_a + V^{-1}_{11}V_{12}\widehat{B}_a \\ \widetilde{B}(\theta)\widehat{D}_a \end{bmatrix} = \begin{bmatrix} \widetilde{B}(\theta)U + Y \\ \widetilde{B}(\theta)U \end{bmatrix}, \\ FC^T_{\varepsilon_{FF}} &= \begin{bmatrix} -\widehat{V}_{11}\widetilde{C}^T(\theta) \\ -W_{11}\widetilde{C}^T(\theta) - Z^T\widetilde{D}^T(\theta) \end{bmatrix}, \\ D_{\varepsilon_{FF}} &= I - \widetilde{D}\widehat{D}_a = I - \widetilde{D}U. \end{aligned} \tag{27}$$

Replacing the LMI items in (26) with (27), we obtain the LMI as in (20). This completes the proof.

(b) It is obvious that $\widehat{G}^*_a(s)$ *as (25) is the solution to (16) if the matrix variables* X, Y, Z, U, W_{11}, *and* $\widehat{V}_{11}$ *are the solution for (19);* W_{12} *and* V_{12}, *could be deduced from (23). This completes the proof.*

Now, the H_∞ optimal inversion feedforward controller which satisfies the optimization problem in (6) can be obtained by Theorem 6.

3.2. Time Domain Implementation of Feedforward Controller. Note that the obtained H_∞ optimal inversion feedforward controller as $\widehat{G}^*_a(s)\widehat{G}_{\mathrm{impr}}(s)$ is improper; it will be realized by preview-based inversion [22]. The design steps are given as follows.

(1) The improper inversion feedforward controller can be transformed to proper form as $\widehat{G}^*_a(s)$ by a transformed desired outputting $\widehat{y}_d(s)$ which carries the preview knowledge of $y_d(s)$. The transformed desired outputting $\widehat{y}_d(s)$ is obtained by multiplying the improper element $\widehat{G}_{\mathrm{impr}}(s)$ and desired outputting $y_d(s)$. The output of feedforward controller $u^*_{\mathrm{FF}}(s)$ is given as follows:

$$\begin{aligned} u^*_{\mathrm{FF}}(s) &= G^*_{\mathrm{FF}}(s)\,y_d(s) = \widehat{G}^*_a(s)\,\widehat{G}_{\mathrm{impr}}(s)\,y_d(s) \\ &= \widehat{G}^*_a(s)\,\widehat{y}_d(s). \end{aligned} \tag{28}$$

(2) By the proper $\widehat{G}^*_a(s)$ and $\widehat{y}_d(s)$, the minimal state space realization of the H_∞ optimal inversion feedforward controller $G^*_{\mathrm{FF}}(s)$ can be given as

$$\begin{aligned} \dot{x}_{\mathrm{FF}}(t) &= A_{\mathrm{FF}}x_{\mathrm{FF}}(t) + B_{\mathrm{FF}}\widehat{y}_d(t), \\ y_{\mathrm{FF}}(t) &= C_{\mathrm{FF}}x_{\mathrm{FF}}(t) + D_{\mathrm{FF}}\widehat{y}_d(t). \end{aligned} \tag{29}$$

(3) Finally, the time domain representation of output of the optimal feedforward controller $u^*_{\mathrm{FF}}(t)$ can be obtained as

$$u^*_{\mathrm{FF}}(t) = C_{\mathrm{FF}}\int_{-\infty}^{t} e^{A_{\mathrm{FF}}(t-\tau)B_{\mathrm{FF}}}\widehat{y}_d(\tau)\,d\tau + D_{\mathrm{FF}}\widehat{y}_d(t). \tag{30}$$

By the above step, the H_∞ optimal inversion is implemented in time domain.

4. Robust Feedback Controller Design

This section will discuss the solution to the robust feedback controller design problem in (7). The H_∞ mixed sensitivity synthesis scheme of 2DOF control system is shown in Figure 2.

By Figure 2, the sensitivity transfer functions of the entire 2DOF control system can be represented as follows:

$$\begin{aligned} S_{\mathrm{2DOF}}(s) &= \left(1 - G_{\mathrm{FF}}(s)G(s)\right)S(s), \\ T_{\mathrm{2DOF}}(s) &= \left(G_{\mathrm{FF}}(s)G(s) + G_{\mathrm{FB}}(s)G(s)\right)S(s). \end{aligned} \tag{31}$$

Integrating with the feedforward which has been determined by design approach proposed in Section 3 and the weighting functions $W_p(s), W_u(s)$, and $W_t(s)$, which impose the requirements for positioning resolution performance, robustness of the entire 2DOF control system, and output signal magnitude of feedback controller, find a feedback controller $G^*_{\mathrm{FB}}(s)$ which could make the optimization problem in (7) satisfied. The design problem of feedback controller could be transformed to seek a controller $G^*_{\mathrm{FB}}(s)$ which could minimize the H_∞ norm of transfer function from desired trajectory y_d to weighting output $T_{y_dZ}(s)$ as in Figure 2; that is,

$$G^*_{\mathrm{FB}}(s) = \min_{G_{\mathrm{FB}}}\sup_{\theta\in\Omega}\left\|T_{y_dZ}(s)\right\|_\infty. \tag{32}$$

The transfer function matrix of P in Figure 2 is given as follows:

$$P(s) = \begin{bmatrix} W_p(s)\left[1 - G(s)G_{\mathrm{FF}}(s)\right] & -W_p(s)G(s) \\ 0 & W_u(s) \\ W_t(s)G(s)G_{\mathrm{FF}}(s) & W_t(s)G(s) \\ 1 - G(s)G_{\mathrm{FF}}(s) & -G(s) \end{bmatrix}. \tag{33}$$

The state space representation of P could be given as

$$\begin{aligned} \dot{x}_p &= A_p(\theta)x_p + B_p(\theta)y_d + B_{p_2}(\theta)u_{\mathrm{FB}}, \\ Z &= C_{p_1}(\theta)x_p + D_{p_{11}}(\theta)y_d + D_{p_{12}}(\theta)u_{\mathrm{FB}}, \\ \varepsilon_{\mathrm{2DOF}} &= C_{p_2}(\theta)x_p + D_{p_{21}}(\theta)y_d. \end{aligned} \tag{34}$$

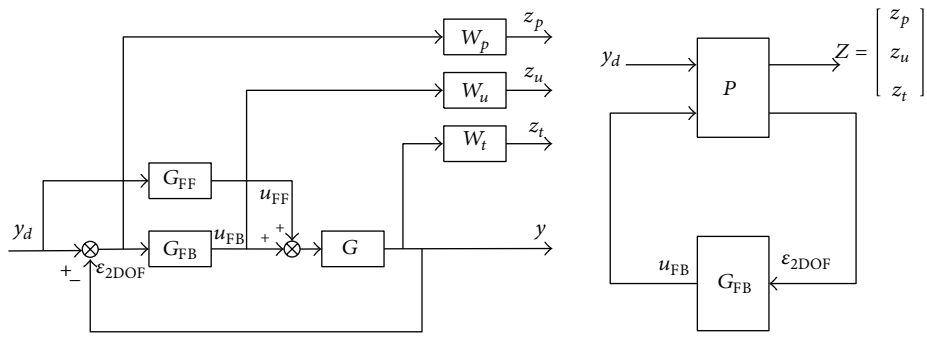

FIGURE 2: H_∞ mixed sensitivity synthesis scheme.

The state space representation of feedback controller G_{FB} is given as follows:

$$\begin{aligned} \dot{x}_{FB} &= A_{FB}x_{FB} + B_{FB}\varepsilon_{2DOF}, \\ u_{FB} &= C_{FB}x_{FB} + D_{FB}\varepsilon_{2DOF}. \end{aligned} \tag{35}$$

Theorem 7. *Consider the system as (34), if there exist symmetric matrices X and Y and matrices with appropriate dimension $\widehat{A}, \widehat{B}, \widehat{C}$, and $\widehat{D}$ that could satisfy the following optimization problem of positive scale γ, that is,*

$$\min_{X,Y,\widehat{A},\widehat{B},\widehat{C},\widehat{D}} (\max(\gamma)) \tag{36}$$

subject to

$$\begin{bmatrix} A_p(\theta)X + XA_p^T(\theta) + B_{p_2}(\theta)\widehat{C} + \left(B_{p_2}(\theta)\widehat{C}\right)^T & \widehat{A}^T + \left(A_p(\theta) + B_{p_2}(\theta)\widehat{D}C_{p_2}(\theta)\right) & B_{p_1}(\theta) + B_{p_2}(\theta)\widehat{D}D_{p_{21}}(\theta) & \left(C_{p_1}(\theta)X + D_{p_{12}}(\theta)\widehat{C}\right)^T \\ * & A_p^T(\theta)Y + YA_p(\theta) + \widehat{B}C_{p_2}(\theta) + \left(\widehat{B}C_{p_2}(\theta)\right)^T & YB_{p_1}(\theta) + \widehat{B}D_{p_{21}}(\theta) & \left(C_{p_1}(\theta) + D_{p_{12}}(\theta)\widehat{D}C_{p_2}(\theta)\right)^T \\ * & * & -\gamma I & \left(D_{p_{11}}(\theta) + D_{p_{12}}(\theta)\widehat{D}D_{p_{21}}(\theta)\right)^T \\ * & * & * & -\gamma I \end{bmatrix} < 0, \quad \begin{bmatrix} X & I \\ I & Y \end{bmatrix} > 0 \tag{37}$$

for $\theta = \theta^* \in \Omega$; the feedback controller which is the solution to the optimization problem

$$\min_{G_{FB}} \sup_{\theta=\theta^*} \left\| T_{y_d Z}(s) \right\|_\infty \tag{38}$$

could be given as

$$\begin{aligned} D_k &= \widehat{D}, \\ C_k &= \left(\widehat{C} - D_k C_{p_2}(\theta^*)X\right)\left(M^T\right)^{-1}, \\ B_k &= N^{-1}\left(\widehat{B} - YB_{p_2}(\theta^*)D_k\right), \\ A_k &= N^{-1}\left[\widehat{A} - Y\left(A(\theta^*) + B_{p_2}(\theta^*)D_k C_{p_2}(\theta^*)\right)X\right] \\ &\quad \cdot \left(M^T\right)^{-1} - B_k C_{p_2}(\theta^*)X\left(M^T\right)^{-1} \\ &\quad - N^{-1}YB_{p_2}(\theta^*)C_k, \end{aligned} \tag{39}$$

where N and M are deduced from $MN^T = I - XY$.

Proof. By BRL and the theorem in [30, 31], there exists a feedback controller such that $\|T_{y_d Z}(s)\|_\infty < \gamma$ for a certain parameter θ^*, if the LMIs in (37) hold, and the feedback controller is given in (39) for a system P with certain parameter θ^*. It is obvious that if there exists a solution of the minimization problem for γ, the feedback controller which is given in (39) is the solution for the minimization problem in (38). This completes the proof. □

Feedback controller G_{FB}^* which satisfies the optimization problem in (7) could be found by the following procedure.

Step 1. Discretize the uncertain parameters θ_i in box domain Ω, set $\theta_{ij} = \theta_{m_i} + (b_i - a_i)(j-1)/m$, $(1 \le j \le m+1;\ m > 1)$, and initialize the parameter vector set $\Theta = \{\Theta_k \mid \Theta_k = (\theta_{1k_1}, \theta_{2k_2}, \ldots, \theta_{qk_q})\}$; $(k_1, k_2, \ldots, k_q \in \{1, 2, \ldots, m\})$; $k \in \{1, 2, k \in \{1, 2, \ldots, m^q\}\}$, $k = 1$.

Step 2. By Theorem 7, obtain the feedback controller G_{FB_k}, which could satisfy the optimization problem $\min_{\Theta_k} \|T_{y_d Z}(s)\|_\infty$ and define $\tau = \min_{\Theta_k} \|T_{y_d Z}(s)\|_\infty$.

Step 3. Define $\lambda_{kl} = \min_{G_{FBk},\Theta_k} \|T_{y_d Z}(s)\|_\infty$. By BRL, we can obtain λ_{kl}. If $\tau < \lambda_{kl}$, for $l \ne k$, $l = 1, 2, \ldots, m^q$, then $G_{FB}^* = G_{FB_k}$ and stop.

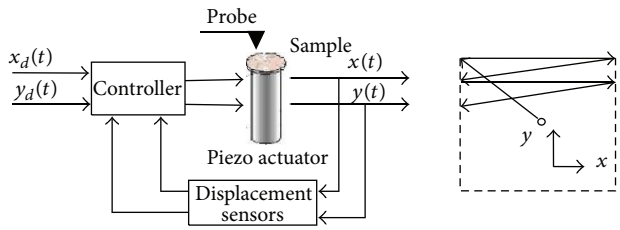

Figure 3: AFM operation diagram and scanning path.

Step 4. Else $k = k + 1$, go to Step 2.

5. Implementation and Experiment

In this section, we will conduct a simulation example of nanopositioning in atomic force microscope (AFM) operation to illustrate the positioning control performance through the proposed 2DOF control design approach.

5.1. Experimental System Description. The AFM system utilizes piezo actuator to enable the x-y axis scanning of the AFM probe relative to the sample surface during AFM imaging as shown in Figure 3. The output error will cause AFM image distortion and sample or probe damaging during scanning. Thus, the positioning control performance of the piezo actuator is important in AFM which measures the surface properties.

To demonstrate the proposed 2DOF control design approach, we will take the x-axis scanning motion control in the simulation experiment in MATLAB Simulink. The model of piezo actuator always is identified by several frequency response measurements. According to frequency response data, an approximate transfer function is obtained, which has parameter uncertainties compared with actual system. Considering the uncertainties, a second-order model of piezo actuator is given as follows [32]:

$$G(s) = \frac{4.019 \times 10^6}{s^2 + \theta_1 s + \theta_2}. \tag{40}$$

The variation bound is given as follows:

$$\theta_{m_i} + \Delta\theta_{i\min} \le \theta_i \le \theta_{m_i} + \Delta\theta_{i\max}, \quad (i = 1, 2), \tag{41}$$

where $\theta_{m_1} = 14.78$, $\Delta\theta_1 \in [0.1, 2]$; $\theta_{m_2} = 2.713 \times 10^5$, $\Delta\theta_2 \in [0.05 \times 10^5, 0.1 \times 10^5]$.

The frequency responses of piezo actuator are shown in Figure 4.

5.2. Design of the Feedforward Controller. The inversion feedforward controller $G_{\mathrm{FF}}(s)$ is selected as follows:

$$G_{\mathrm{FF}}(s) = a^*(s)\,\widehat{G}(s) = \widehat{G}_a^*(s)\,\widehat{G}_{\mathrm{impr}}(s). \tag{42}$$

The improper element $\widehat{G}_{\mathrm{impr}}(s)$ could be written as

$$\widehat{G}_{\mathrm{impr}}(s) = \frac{s^2 + 14.78s + 2.713 \times 10^5}{4.019 \times 10^6}. \tag{43}$$

The transfer function $\widetilde{G}(s)$ in (11) and its state matrices in (12) could be given as follows:

$$\begin{aligned}
\widetilde{G}(s) &= \widehat{G}_{\mathrm{impr}}(s)\,G(s) = \frac{s^2 + 14.78s + 2.713 \times 10^5}{s^2 + \theta_1 s + \theta_2}, \\
\widetilde{A} &= \begin{bmatrix} 0 & 1 \\ -\left(2.713 \times 10^5 + \Delta\theta_2\right) & -\left(14.78 + \Delta\theta_1\right) \end{bmatrix}, \\
\widetilde{B} &= \begin{bmatrix} 0 \\ 1 \end{bmatrix}, \\
\widetilde{C} &= \left[-\Delta\theta_2 \quad -\Delta\theta_1\right], \\
\widetilde{D} &= 1.
\end{aligned} \tag{44}$$

By using Theorem 6 and LMI toolbox in MATLAB, the H_∞ optimal inversion feedforward controller is obtained as follows which could render

$$\begin{aligned}
G_{\mathrm{FF}}^*(s) = \widehat{G}_a^*(s)\,\widehat{G}_{\mathrm{impr}}(s) &= \left(\frac{0.9979s + 0.0188}{s + 0.0287}\right) \\
&\cdot \left(\frac{s^2 + 14.78s + 2.713 \times 10^5}{4.019 \times 10^6}\right).
\end{aligned} \tag{45}$$

The output of H_∞ optimal inversion feedforward controller u_{FF}^* could be obtained by the obtained $G_{\mathrm{FF}}^*(s)$ and preview inversion design steps as in (28)–(30).

5.3. Design of the Feedback Controller. At first, we specify the weighting function. It is noted that the tracking error could be achieved to around 30% by H_∞ optimal inversion feedforward controller. We chose the weighting function for control bandwidth and positioning error limitation as $W_p(s) = 80/(1 + 0.01s)$ which specifies the positioning error to be less than 2.5% below frequency at 125 Hz. The frequency response of $W_p(s)$ is shown in Figure 5.

Considering system robustness requirement and the parameter uncertainty domain, the weighting function for system robustness performance is chosen as $W_t(s) = (s + 1)/(10s + 8)$. The frequency response of $W_t(s)$ is shown in Figure 6.

Considering the limitation of the controller output signal, the weighting function for magnitude of output signal of feedback controller is chosen to be a constant, $W_u(s) = 1/50$.

Through design procedure of robust feedback controller and selecting $\tau = 0.2$, we obtained the feedback controller by using LMI toolbox in MATLAB. It is given as follows:

$$G_{\mathrm{FB}} = \frac{p_{\mathrm{FB}}(s)}{n_{\mathrm{FB}}(s)}, \tag{46}$$

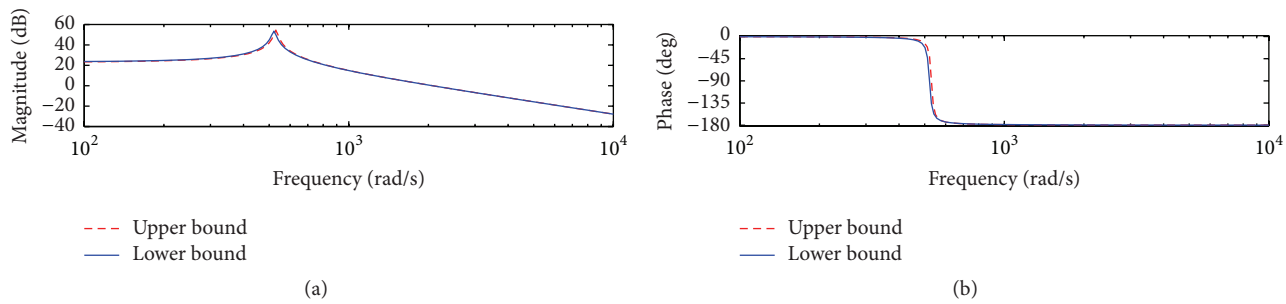

Figure 4: The frequency response of piezo actuator.

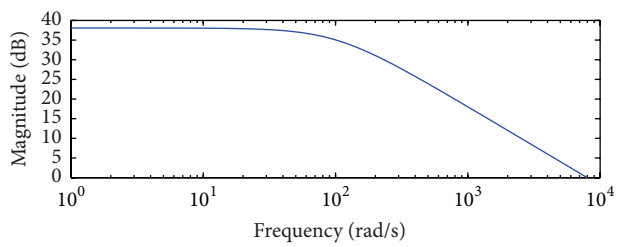

Figure 5: The frequency response of $W_p(s)$.

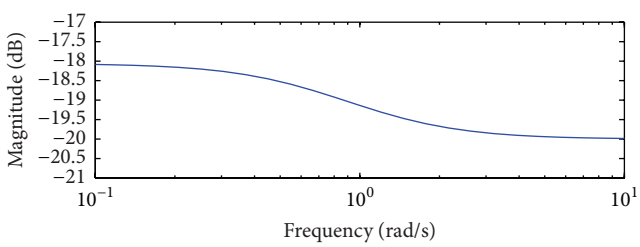

Figure 6: The frequency response of $W_t(s)$.

where

$$\begin{aligned} p_{\mathrm{FB}}(s) &= 11.76s^6 + 4.10\times10^7 s^5 + 3.47\times10^{11}s^4 \\ &\quad + 9.81\times10^{14}s^3 + 1.08\times10^{15}s^2 + 2.36 \\ &\quad \times10^{14}s + 130.4, \\ n_{\mathrm{FB}}(s) &= s^6 + 2.40\times10^5 s^5 + 1.04\times10^{10}s^4 + 4.67 \\ &\quad \times10^{12}s^3 + 7.61\times10^{11}s^2 + 1.81\times10^{10}s \\ &\quad + 5.59. \end{aligned} \tag{47}$$

By H_∞ mixed sensitivity design approach without considering the feedforward controller and the above-selected weighting function, we obtained the controller by using MATLAB H_∞ mixed sensitivity synthesis command "hinf". It is given as follows:

$$G_H = \frac{2.63\times10^6 s^3 + 4.09\times10^7 s^2 + 7.12\times10^{11}s + 5.70\times10^{11}}{s^4 + 7.35\times10^4 s^3 + 1.32\times10^9 s^2 + 1.32\times10^{11}s + 1.05\times10^{11}}. \tag{48}$$

Table 1: Comparison of positioning control error.

Frequency	$e_{\max}$ (um)			E_{mean} (um)		
	(1)	(2)	(3)	(1)	(2)	(3)
5 HZ	0.0019	0.0027	0.0138	0.0002	0.0003	0.0073
50 HZ	0.0034	0.0061	0.0258	0.0003	0.0034	0.0148
125 HZ	0.0057	0.0103	0.0447	0.0008	0.0054	0.0303

5.4. Experiment and Result Discussion. The AFM x-axis positioning control simulation experiment which is tracking triangular trajectory at three different frequencies (5 Hz, 50 Hz, and 125 Hz) was conducted. For comparison, the positioning performances of three control approaches were tested by simulation experiment. The approaches are as follows: (1) the proposed H_∞ optimal inversion feedforward and robust feedback 2DOF control approach, that is, $(G^*_{\mathrm{FF}} + G^*_{\mathrm{FB}})$, (2) exact inversion feedforward-robust feedback based 2DOF control approach, that is, $(G_{\mathrm{FF}m} + G_H)$, and (3) H_∞ mixed sensitivity feedback control only, that is, G_H. The positioning control performance was evaluated by positioning maximum error and mean error, which are described as follows:

$$\begin{aligned} e_{\max} &= \max_{k\in[1,n]} \left(y_d(k) - y(k)\right), \\ E_{\mathrm{mean}} &= \sqrt{\frac{\sum_{k=1}^{n}\left(y_d(k) - y(k)\right)^2}{n}}. \end{aligned} \tag{49}$$

Figure 7 shows the positioning control simulation results and positioning errors by using different control approaches. The maximum positioning errors and mean errors for triangular trajectory scanning at different frequencies are shown in Table 1. The range of triangular trajectory was 1 μm. As shown, at scan rate 5 Hz, these three control approaches could achieve precision positioning; maximum positioning errors are 0.0019 μm, 0.0027 μm, and 0.0138 μm, respectively, and mean positioning errors are 0.0002 μm, 0.0003 μm, and 0.0073 μm, respectively. At scan rate 50 Hz, the proposed 2DOF control approach and the exact inversion feedforward and robust feedback based 2DOF control approach could obtain a better positioning control performance than H_∞ mixed sensitivity feedback control only. The maximum positioning errors obtained by approaches (1) and (2) are 0.0034 μm and 0.0061 μm which are as small as 13.2% and

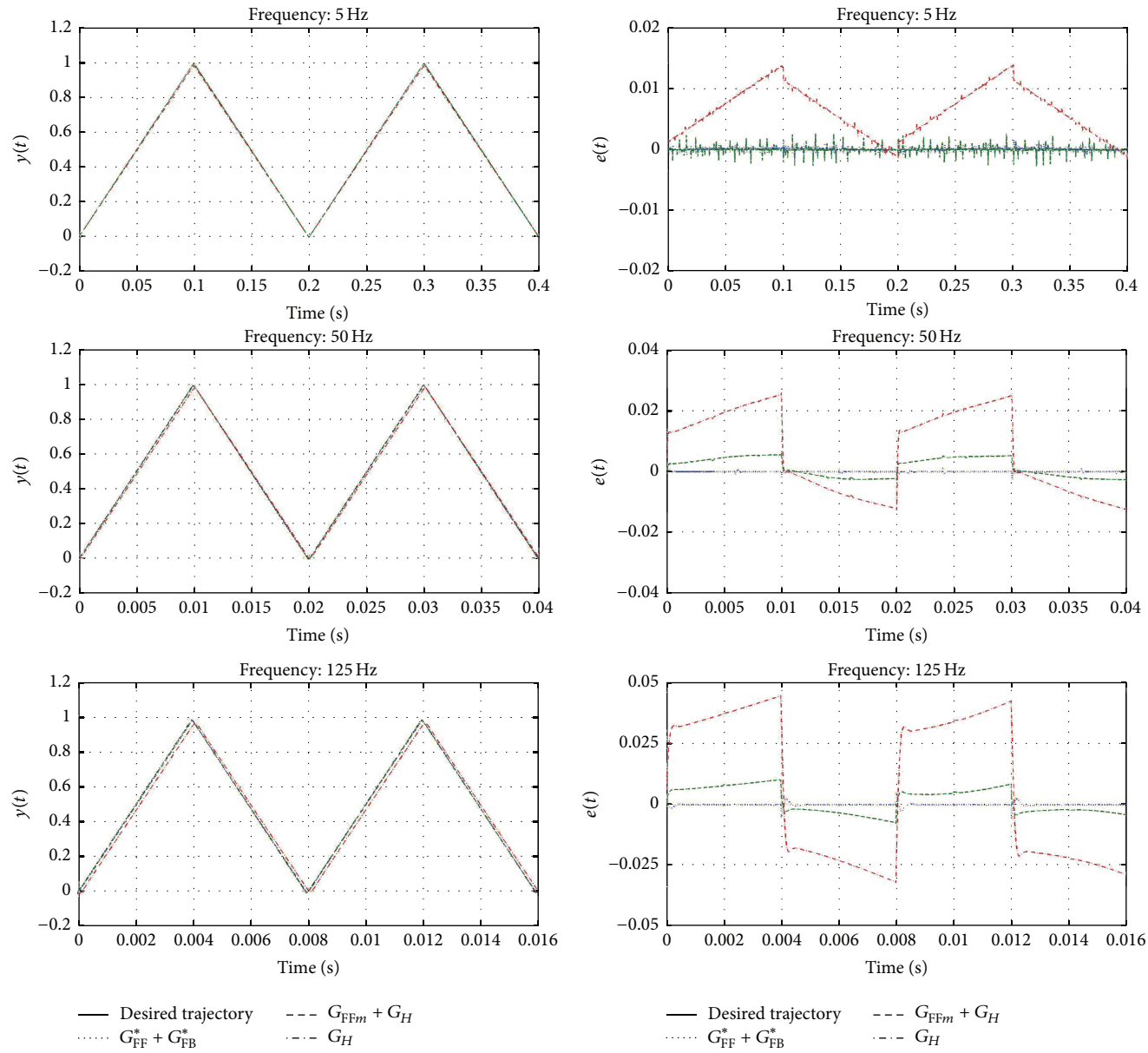

Figure 7: AFM x-axis positioning control simulation experiment result.

23.6% of that obtained by H_∞ mixed sensitivity feedback control. The positioning mean errors obtained by approaches (1) and (2) are 0.0003 μm and 0.0034 μm which are as small as 2% and 22% of that obtained by approach (3). At scan rate 125 Hz, only the proposed 2DOF control could obtain precision positioning. The maximum positioning error obtained by approach (1) is 0.0057 μm, which is as small as 55% of that obtain by approach (2) and is as small as 12.7% of that obtain by approach (3). The positioning mean error obtained by approach (1) is 0.0008 μm, which is as small as 14.8% of that obtained by approach (2) and is as small as 2.6% of that obtained by approach (3). Through the experiment result analysis, it is obvious that the proposed 2DOF control could achieve better positioning precision than the other two control approaches both in high speed scanning.

6. Conclusion

In this paper, a novel H_∞ optimal inversion feedforward and robust feedback based 2DOF control approach for high speed-precision positioning systems is proposed. In this approach, an H_∞ optimal inversion feedforward controller is designed to minimize the H_∞ norm of the tracking error in the presence of model uncertainty via linear matrix inequality (LMI) synthesis. Integrating with the feedforward controller systematically, a robust feedback controller is designed to render the requirements of positioning resolution, control width, robustness, and output signal magnitude imposed on the entire 2DOF control system satisfied via LMI optimization. The proposed control design approach is implemented in an AFM system x-axis positioning simulation experiment,

and the experiment results demonstrated the effectiveness of the proposed 2DOF control approach.

Conflict of Interests

The authors declare that there is no conflict of interests regarding the publication of this paper.

Acknowledgment

This work is supported by China Postdoctoral Science Foundation under Grant 2014M560710.

References

[1] J.-C. Shen, W.-Y. Jywe, H.-K. Chiang, and Y.-L. Shu, "Precision tracking control of a piezoelectric-actuated system," *Precision Engineering*, vol. 32, no. 2, pp. 71–78, 2008.

[2] G. Schitter, F. Allgöwer, and A. Stemmer, "A new control strategy for high-speed atomic force microscopy," *Nanotechnology*, vol. 15, no. 1, pp. 108–114, 2004.

[3] M.-Y. Chen and J.-S. Lu, "High-precision motion control for a linear permanent magnet iron core synchronous motor drive in position platform," *IEEE Transactions on Industrial Informatics*, vol. 10, no. 1, pp. 99–108, 2014.

[4] B. E. Helfrich, C. Lee, D. A. Bristow et al., "Combined H_∞-feedback control and iterative learning control design with application to nanopositioning systems," *IEEE Transactions on Control Systems Technology*, vol. 18, no. 2, pp. 336–351, 2010.

[5] K. Yang, Y. Choi, and W. K. Chung, "On the tracking performance improvement of optical disk drive servo systems using error-based disturbance observer," *IEEE Transactions on Industrial Electronics*, vol. 52, no. 1, pp. 270–279, 2005.

[6] C. Du, L. Xie, J. N. Teoh, and G. Guo, "An improved mixed H_2/H_∞ control design for hard disk drives," *IEEE Transactions on Control Systems Technology*, vol. 13, no. 5, pp. 832–839, 2005.

[7] Z. Z. Liu, F. L. Luo, and M. A. Rahman, "Robust and precision motion control system of linear-motor direct drive for high-speed X-Y table positioning mechanism," *IEEE Transactions on Industrial Electronics*, vol. 52, no. 5, pp. 1357–1363, 2005.

[8] B. Yao and L. Xu, "Adaptive robust motion control of linear motors for precision manufacturing," *Mechatronics*, vol. 12, no. 4, pp. 595–616, 2002.

[9] A. C. Shegaonkar and S. M. Salapaka, "Making high resolution positioning independent of scan rates: a feedback approach," *Applied Physics Letters*, vol. 91, no. 20, Article ID 203513, 2007.

[10] J. S. Freudenberg, C. V. Hollot, R. H. Middleton, and V. Toochinda, "Fundamental design limitations of the general control configuration," *IEEE Transactions on Automatic Control*, vol. 48, no. 8, pp. 1355–1370, 2003.

[11] A. Karimi, M. Kunze, and R. Longchamp, "Robust controller design by linear programming with application to a double-axis positioning system," *Control Engineering Practice*, vol. 15, no. 2, pp. 197–208, 2007.

[12] T. Uchihashi, N. Kodera, H. Itoh, H. Yamashita, and T. Ando, "Feed-forward compensation for high-speed atomic force microscopy imaging of biomolecules," *Japanese Journal of Applied Physics*, vol. 45, no. 3, pp. 1904–1908, 2006.

[13] D. Croft and S. Devasia, "Vibration compensation for high speed scanning tunneling microscopy," *Review of Scientific Instruments*, vol. 70, no. 12, pp. 4600–4605, 1999.

[14] C. Lee, G. Mohan, and S. Salapaka, "2DOF control design for nanopositioning," in *Control Technologies for Emerging Micro and Nanoscale Systems*, vol. 413 of *Lecture Notes in Control and Information Sciences*, pp. 67–82, Springer, Berlin, Germany, 2011.

[15] G. Schitter, A. Stemmer, and F. Allgower, "Robust two-degree-of-freedom control of an atomic force microscope," *Asian Journal of Control*, vol. 6, no. 2, pp. 156–163, 2004.

[16] C. Lee and S. M. Salapaka, "Robust broadband nanopositioning: fundamental trade-offs, analysis, and design in a two-degree-of-freedom control framework," *Nanotechnology*, vol. 20, no. 3, Article ID 035501, 2009.

[17] K. Takanori, M. Yoshihiro, and I. Makoto, "LMI-based 2-degree-of-freedom controller design for robust vibration suppression positioning," *IEEJ Transactions on Industry Application*, vol. 131, no. 1, pp. 93–101, 2011.

[18] M. Araki and H. Taguchi, "Two-degree-of-freedom PID controllers," *International Journal of Control, Automation, and Systems*, vol. 1, no. 4, pp. 401–411, 2003.

[19] S. Devasia, D. Chen, and B. Paden, "Nonlinear inversion-based output tracking," *IEEE Transactions on Automatic Control*, vol. 41, no. 7, pp. 930–942, 1996.

[20] L. R. Hunt, G. Meyer, and R. Su, "Noncausal inverses for linear systems," *IEEE Transactions on Automatic Control*, vol. 41, no. 4, pp. 608–611, 1996.

[21] S. Devasia and B. Paden, "Stable inversion for nonlinear nonminimum phase time-varying system," *IEEE Transactions on Automatic Control*, vol. 43, no. 2, pp. 283–288, 1998.

[22] Q. Zou and S. Devasia, "Preview-based optimal inversion for output tracking: application to scanning tunneling microscopy," *IEEE Transactions on Control Systems Technology*, vol. 12, no. 3, pp. 375–386, 2004.

[23] Y. Yan, Y. Wu, Q. Zou, and C. Su, "An integrated approach to piezoactuator positioning in high-speed atomic force microscope imaging," *Review of Scientific Instruments*, vol. 79, no. 7, Article ID 073704, 9 pages, 2008.

[24] S. Devasia, "Should model-based inverse inputs be used as feedforward under plant uncertainty?" *IEEE Transactions on Automatic Control*, vol. 47, no. 11, pp. 1865–1871, 2002.

[25] Q. Zou, K. K. Leang, and E. Sadoun, "Control issues in high-speed AFM for biological applications: collagen imaging example," *Asian Journal of Control*, vol. 6, no. 2, pp. 164–178, 2004.

[26] C. G. L. Bianco and A. Piazzi, "A servo control system design using dynamic inversion," *Control Engineering Practice*, vol. 10, no. 8, pp. 847–855, 2002.

[27] K. K. Leang and S. Devasia, "Feedback-linearized inverse feedforward for creep, hysteresis, and vibration compensation in AFM piezoactuators," *IEEE Transactions on Control Systems Technology*, vol. 15, no. 5, pp. 927–935, 2007.

[28] M. Tahk and J. L. Speyer, "Modeling of parameter variations and asymptotic LQG synthesis," *IEEE Transactions on Automatic Control*, vol. 32, no. 9, pp. 793–801, 1987.

[29] G. Chesi, "Estimating the domain of attraction for uncertain polynomial systems," *Automatica*, vol. 40, no. 11, pp. 1981–1986, 2004.

[30] Y. He, M. Wu, and J.-H. She, "Improved bounded-real-lemma representation and H_∞ control of systems with polytopic uncertainties," *IEEE Transactions on Circuits and Systems II: Express Briefs*, vol. 52, no. 7, pp. 380–383, 2005.

[31] M.-N. Lee, J.-H. Moon, K. B. Jin, and M. J. Chung, "Robust H_∞ control with multiple constraints for the track-following system of an optical disk drive," *IEEE Transactions on Industrial Electronics*, vol. 45, no. 4, pp. 638–645, 1998.

[32] Q. Xu and Y. Li, "Model predictive discrete-time sliding mode control of a nanopositioning piezostage without modeling hysteresis," *IEEE Transactions on Control Systems Technology*, vol. 20, no. 4, pp. 983–994, 2012.